Ocean Systems Engineering, *Vol. 8, No. 3 (2018) 345-360*
DOI: https:// doi.org/10.12989/ose.2018.8.3.345

Mathieu stability of offshore Buoyant Leg Storage & Regasification Platform

S. Chandrasekaran* and P.A. Kiran

Department of Ocean Engg., Indian Institute of Technology Madras, India

(Received February 27, 2018, Revised June 29, 2018, Accepted July 27, 2018)

Abstract. Increasing demand for large-sized Floating, Storage and Regasification Units (FSRUs) for oil and gas industries led to the development of novel geometric form of Buoyant Leg Storage and Regasification Platform (BLSRP). Six buoyant legs support the deck and are placed symmetric with respect to wave direction. Circular deck is connected to buoyant legs using hinged joints, which restrain transfer of rotation from the legs to deck and vice-versa. Buoyant legs are connected to seabed using taut-moored system with high initial pretension, enabling rigid body motion in vertical plane. Encountered environmental loads induce dynamic tether tension variations, which in turn affect stability of the platform. Postulated failure cases, created by placing eccentric loads at different locations resulted in dynamic tether tension variation; chaotic nature of tension variation is also observed in few cases. A detailed numerical analysis is carried out for BLSRP using Mathieu equation of stability. Increase in the magnitude of eccentric load and its position influences fatigue life of tethers significantly. Fatigue life decreases with the increase in the amplitude of tension variation in tethers. Very low fatigue life of tethers under Mathieu instability proves the severity of instability.

Keywords: offshore platforms; Mathieu stability; dynamic tether tension; eccentric loading

1. Introduction

Increasing demand for larger storage and regasification floating units to transport liquefied natural gas (LNG) results in exploration of offshore processing platforms in recent past; new geometrical form of BLSRP is proposed to meet increasing functional requirements (Chandrasekaran and loganath 2015, 2017). Circular deck, used for storage and processing LNG is supported on six buoyant legs, which are symmetrically positioned with respect to center of gravity of the deck. This arrangement makes the platform insensitive to wave directionality. Hinged joints, which connect the legs and buoyant legs, isolate the deck partially. Buoyant leg structures show a few major advantages namely: easy installation, transportation, fabrication and technical superiority (Graham *et al.* 1980, Robert *et al.* 1995, Chandrasekaran *et al*. 2015a, Chandrasekaran *et al.* 2015b). Uniqueness of BLSRP is partial isolation of the deck from buoyant legs, which reduces the deck response in rotational degrees-of-freedom, making it safe for LNG

∗Corresponding author, Professor, E-mail: drsekaran@iitm.ac.in
[a] Senior research scholar, E-mail: kiranpajith@yahoo.com

http://www.techno-press.org/?journal=ose&subpage=7 ISSN: 2093-6702 (Print), 2093-677X (Online)

processing (White *et al.* 2005, Chandresekaran *et al*. 2011, 2013, Chandrasekaran and Madhuri 2012a, b, 2013, 2015). Considerable reduction in deck response compared to buoyant legs in all degrees of freedom is noted under regular and random waves, making this new geometry suitable for deep waters. Even though rotational degrees of freedom is not transferred to the deck, pitch response is noted in the deck due to the differential heave in the buoyant legs. As the platform is positive-buoyant, high initial pretension on tethers is necessary to ensure position restraint (Chandrasekaran *et al*. 2010). Buoyant legs and tethers are inclined at 20 degree angle to the vertical plane of the deck using spread taut mooring system.

Detailed investigations on compliant platforms like Spar (Haslum and Faltinsen 1999, Koo *et al.* 2004) showed Mathieu-type instability in systems where pitch natural period is about twice as that of heave. Dynamic behavior under unstable conditions showed chaotic behavior, which is critical to ensure safe functionality of the platform (Rho *et al.* 2002, 2003, 2004, 2005, Adrain *et al.* 2013). Mathieu stability analysis of TLP tethers was investigated considering tether as a simply supported column with constant tension along its length, excluding the nonlinear damping term and by using Galerkin's method the governing equation was cut down to Mathieu equation (Jeffreys and Patel 1982). Using perturbation method and Runge-Kuttta method, Mathieu stability charts were extended to large parameters since TLPs exhibits large values for Mathieu parameters (Goldstein 1929, Ince 1925). Stability analysis, based on the extended chart showed the necessity of Mathieu stability study in tethers (Patel and Park 1991).Recent studies proposed dynamic model for Mathieu equation of TLP tethers under lateral vibration. This model uses linear, cable equation, considering tension variation in the cable due to submerged mass (Simos and Pesce 1991). Stability analysis of Auger TLP and Hutton TLP showed that the platforms underwent Mathieu type instability, which resulted in their failure, which was subsequently repaired and corrected (Chandrasekaran *et al*. 2006, Mclachlan 1947).

Tension leg platforms which are taut moored undergo Mathieu type instability due to the dynamic tether tension variation under wave forces and spar platforms undergo Mathieu type instability due to coupling of heave and pitch motions when the pitch natural frequency is twice that of heave natural frequency. Since Buoyant leg storage regasification platform inherits features of both TLP and spar, they may be prone to Mathieu type instability. Tethers play a significant role in stability of taut moored compliant structures and hence understanding tether stability is important. Literature review lacks stability analysis of this new generation platforms and hence it's vital to conduct stability analysis of these new geometric forms.

2. Formulation of mathieu equation

Dynamic equation of tether is formulated using an idealized linear model, which is a straight slender column simply supported at ends (Simos and Pesce 1997). Tension due to submerged mass is considered to be linearly varied along its length. Dynamic equation of tether vibration is formulated using an idealized linear model. This is similar to that of straight slender column, which is simply supported at ends under varying axial tension caused due to its varying submerged mass. Ignoring flexural rigidity and current effects, dynamic equation for the lateral movement of tether is given by

$$M\frac{\partial^2 y}{\partial t^2} - \frac{\partial}{\partial x}\left[T(x).\frac{\partial y}{\partial x}\right] + Bv\left|\frac{\partial y}{\partial t}\right|.\frac{\partial y}{\partial t} = 0 \tag{1}$$

Where, M is the total mass of the tether, which is the sum of added mass and physical mass per unit length. T(x) is the total tension in the tether, which is the sum of static tension and dynamic tension given by

$$T(x) = P + \mu g(L - x) - Acos(\omega t) \tag{2}$$

P is the initial pretension in the tethers, μ is the mass per unit length of the tether, L is tether length, A is the tension amplitude, ω is the wave frequency, Bv is the viscous damping coefficient.
For free lateral vibration of tether, Eq. (2) becomes

$$M\frac{\partial^2 y}{\partial t^2} - \frac{\partial T(x)}{\partial x} = 0 \tag{3}$$

Lateral motion of nth natural mode is assumed as

$$y_n\,(X_n t) = f_n(t).X_n(x) \tag{4}$$

Substituting (4) in (1) we get a classical Sturm-Liouville problem

$$\left(\left[\frac{P}{M} + \frac{\mu g(L-x)}{M}\right] X_n\right) + \omega_n{}^2 X_n = 0 \tag{5}$$

The above equation can be rewritten by introducing a new variable η and after some algebraic work the Eq. (5) becomes a modified Bessel equation

$$\eta^2 X_n + \eta X_n + 4\boldsymbol{\beta}_n{}^2\, \eta^{\,2} X_n = 0 \tag{6}$$

Where

$$\eta = \sqrt{1 + \frac{\mu g(L-x)}{P}} \tag{7}$$

$$\beta_n{}^2 = \frac{(\mu g)^2}{PM}\omega_n{}^2 \tag{8}$$

Solution for Eq. (6) is obtained in Bessel functions (J_0,Y_0) (Bowman 1958) and is obtained as

$$X_n(n) = C_1\, J_0\,(2\,\boldsymbol{\beta}_n\,\eta) + C_2\, Y_0\,(2\boldsymbol{\beta}_n\,\eta) \tag{9}$$

By applying boundary conditions

$$X_n\,(\,\eta\,|\tau = 0\,) = 0 \text{ and } X_n\,(\,\eta\,|\tau = 1\,) = 0 \tag{10}$$

The constants are obtained and the Eq. (9) for the resultant modal forms, is obtained as below

$$X_n(x)=J_0\left(2\beta_n\left[1 + \frac{\mu g(L-x)}{P}\right]^{1/2}\right) - \frac{J_0(2\beta n)}{Y_0(2\beta n)}\, Y_0\left(2\beta_n\left[1 + \frac{\mu g(L-x)}{P}\right]^{1/2}\right) \tag{11}$$

Where, $\boldsymbol{\beta}_n$ is obtained as the solution of the equation given below

$$J_0\left(2\beta_n\sqrt{1 + \frac{\mu gL}{P}}\right) Y_0\,(2\boldsymbol{\beta}_n) - Y_0\left(2\beta n\sqrt{1 + \frac{\mu gL}{P}}\right) J_0\,(2\boldsymbol{\beta}_n) = 0 \tag{12}$$

By substituting Eq. (11) in Eq. (1) and applying Galerkin's variation method, the Eq. (1) is re-written as

$$\frac{d^2f}{d\tau} + (\boldsymbol{\delta} - \mathbf{q}\cos(2\boldsymbol{\tau}))f + c\left|\frac{df}{d\tau}\right|\frac{df}{d\tau} = 0 \tag{13}$$

Where, $2\boldsymbol{\tau} = \omega t$ ($\boldsymbol{\tau}$ dimensionless time variable) and f is the lateral displacement of tether. $\boldsymbol{\delta}$ and q are Mathieu parameters given by

$$\boldsymbol{\delta}_n = \frac{4}{M\omega^2}\left\{\mu g\frac{(I_2 + I_4)}{I_1}\right\} - (P + \mu g L)\frac{I_3}{I_1} \tag{14a}$$

$$q_n = \frac{2a}{M\omega^2}\frac{I_3}{I_1} \tag{14b}$$

where, M is the total tether mass, ω is the wave frequency, μ is the mass per unit length of tether, g is acceleration due to gravity, P is the initial pretension and a is the tension amplitude. Corresponding integrals of the above equations are given by

$$I_1 = \int_0^L {X_n}^2(x)dx \tag{15a}$$

$$I_2 = \int_0^L \frac{dX_n(x)}{dx}dx \tag{15b}$$

$$I_3 = \int_0^L \frac{d^2X_n(x)}{dx^2}X_n(x)\,dx \tag{15c}$$

$$I_4 = \int_0^L \frac{d^2X_n(x)}{dx^2}X_n(x)dx \tag{15d}$$

As stability condition is influenced by Mathieu parameters, solution to Mathieu equation is expressed in the form of a stability chart.

3. Numerical modeling

Numerical analysis of offshore triceratops and Buoyant Leg Storage and Regasification Platform for hydrodynamic response and dynamic tether tension variation are carried out using ANSYS AQWA software. The geometric propertied are derived from existing TLP (Chandrasekaran and Jain 2000), keeping the total mass, buoyancy force, initial pretension in tethers and total deck area same as that of TLP. As buoyant legs qualify for Morison region, they are modeled using line elements in ANSYS AQWA workbench. Each buoyant leg is further assigned with outer diameter 14.14 m and wall thickness of 0.15 m. The mass of the buoyant leg structure (BLS) units, ballast load and weight of the deck are assigned to the mass center on the vertical plane. The radii of gyration about three translational axes are designed in ANSYS design modular. Each buoyant leg unit is modeled as an independent rigid body as they are not interconnected. Deck consists of quadrilateral and triangular plate elements with appropriate mass properties. Buoyant legs are connected to the deck using ball joints (Chandrasekaran 2015, 2016, 2017, Chandrasekaran and Jain 2016). Tethers, those extend form keel of the buoyant leg to sea bed, are modeled as flexible elements. Buoyant legs are connected to the sea bed with groups of tethers containing four tethers in each group. Each leg consists of a group of 4 tethers and a total of 24 tethers hold-down the platform under a spread-mooring system. Fig. 1 shows the numerical model under moored condition, which is referred as normal case in the analysis. Static equilibrium between the buoyancy force, weight and initial tether tension is given as below

$$F_b = W + 6\,T_0 \cos(20) \tag{16}$$

It is important to note that a maximum inclination of 20° with respect to the vertical is allowed for the legs and the downward force due to pretension of tethers is the vertical component of tether force given by $T_0\cos(20)$, Fb is the total buoyant force and W is the total weight of the structure . Table 1 shows the geometric properties of the platform. Three cases under eccentric loads are analyzed namely: i) eccentric load on top of one buoyant leg (referred as case 2); ii) eccentric load in between two adjacent buoyant legs (referred as case 3); and iii) eccentric load on top of two adjacent buoyant legs (referred as case 4). Such cases of eccentric loading are accidental and hence referred as postulated failure cases in the study. Fig. 2 shows the numerical model with different position of eccentric loads. Each case of eccentric loading is analyzed for two load magnitudes namely: 5% and 10% of that of the total mass.

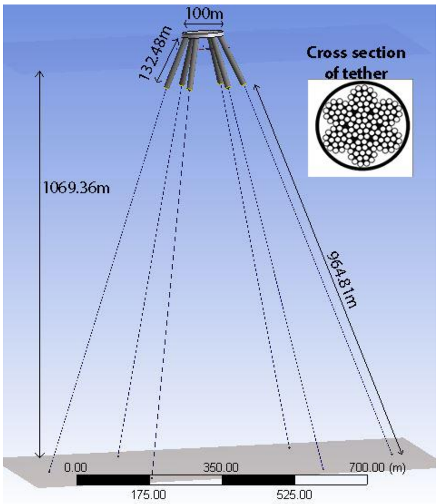

Fig. 1 Numerical model of BLSRP (normal case)

Table 1 Geometric properties of platform

Description	BLSRP
Water depth	1069.36 m
Total weight	641000 kN
Buoyant force	940880 kN
Diameter of buoyant leg	14.14 m
Diameter of deck	99.40 m
Length of buoyant leg	132.48 m
Total tether force	319125.60 kN
Pretension in each leg	53187.61 kN
Tether length	964.81 m
Number of tethers (6 groups)	24
Axial stiffness of tethers	76830.67 kN/m

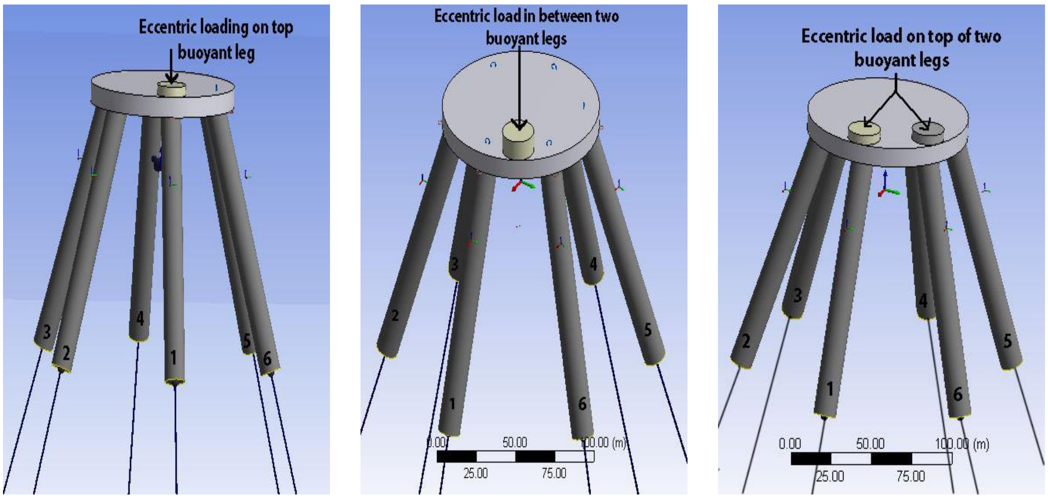

Fig. 2 Numerical model of BLSRP under postulated failure i) case 2; ii) case 3; iii) case 4

4. Results and discussions

BLSRP is analyzed under regular wave of wave height 5 m and time period 6.8 s taken from literature for Gulf of Mexico (Chandrasekaran *et al.* 2006, Simos and Pesce 1991) under zero degree incident angle to BLS 1, under normal and postulated failure cases. BLSRP under eccentric loading is analyzed for two loads 32050 kN (5%) and 64100 kN (10%) as 15% or more of payload on center of gravity of the deck causes instability in the structure (Chandrasekaran and Kiran 2017). The presence of eccentric loading causes offset in the heave degree of freedom (Fig. 3), reducing the pretension in tethers near the eccentric loading causing more response in buoyant legs. Maximum tension amplitude is summarized in Table 2 while dynamic tether tension variations, for a postulated failure cases are shown in Fig. 4.

Table 2 Maximum tension amplitude in tethers under postulated failure cases

Description	Load	Leg 1 (MN)	Leg 2 (MN)	Leg 3 (MN)	Leg 4 (MN)	Leg 5 (MN)	Leg 6 (MN)	Maximum (MN)
Case 1	-	62.49	61.53	61.43	61.40	61.85	60.97	62.49
Case 2	5%	89.99	71.78	59.08	63.56	65.76	73.70	89.99
	10%`	168.54	140.70	76.40	128.80	80.79	136.04	168.54
Case 3	5%	85.06	18.52	68.28	67.98	65.11	77.17	85.06
	10%`	153.42	112.99	103.06	100.50	110.26	144.23	153.42
Case 4	5%	82.34	64.45	64.91	64.57	63.22	69.21	82.34
	10%`	112.36	99.39	73.37	68.76	80.14	107.94	112.36

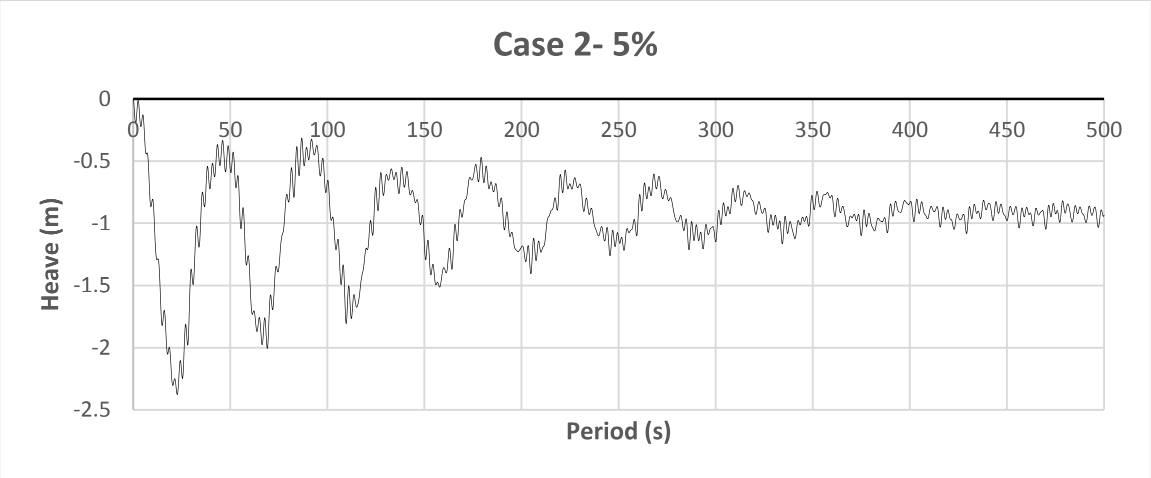
Case 2- 5%
0
-0.5
-1
-1.5
-2
-2.5
Heave (m)
0
50
100
150
200
250
300
350
400
450
500
Period (s)

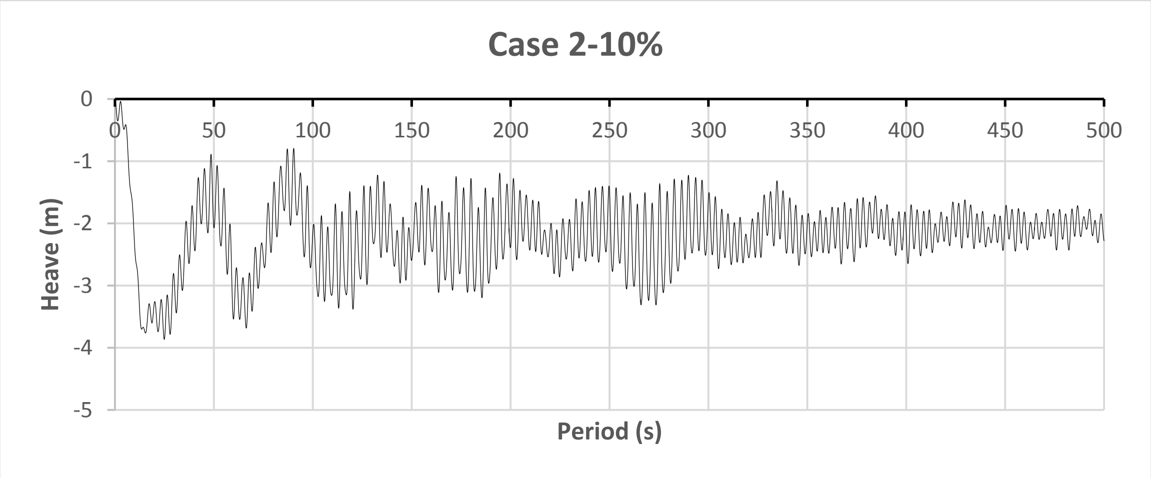
Case 2-10%
0
-1
-2
-3
-4
-5
Heave (m)
0
50
100
150
200
250
300
350
400
450
500
Period (s)

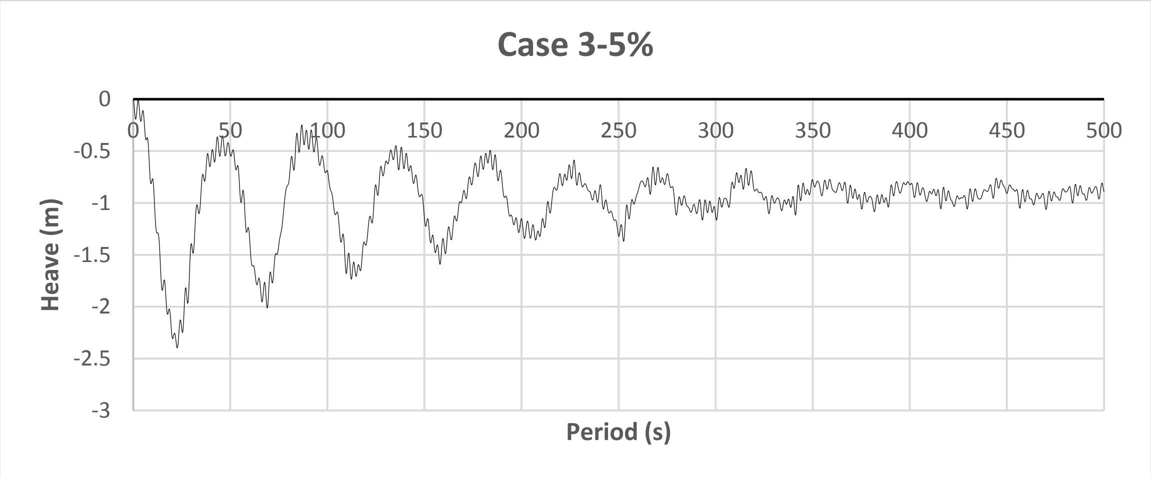
Case 3-5%
0
-0.5
-1
-1.5
-2
-2.5
-3
Heave (m)
0
50
100
150
200
250
300
350
400
450
500
Period (s)

Continued-

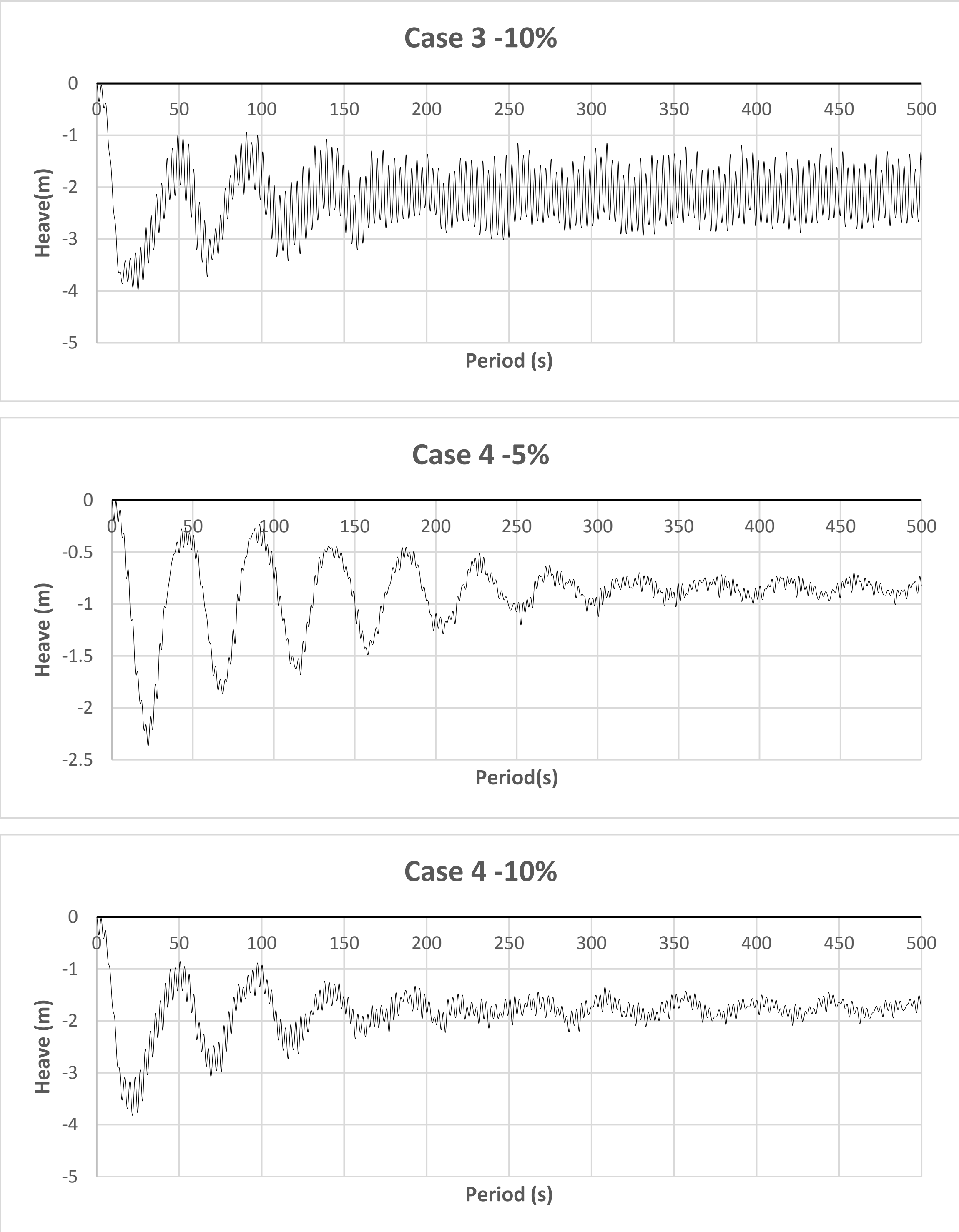

Fig. 3 Heave response of the deck under postulated failure cases

Postulated failure cases, created by placing eccentric loads at different locations resulted in dynamic tether tension variation given in Fig. 4. Each case is examined for Mathieu type instability. For the known values of initial pretension, length, cross-section area, total mass of platform and submerged mass of tethers, natural period of tethers are obtained analytically to determine lateral motion of tethers. Substituting the lateral motion obtained analytically and tether tension variation obtained numerically, Mathieu parameters derived for the tether equation of motion are obtained for first mode of vibration. Parameters are then plotted in Mathieu stability chart to obtain stability of the structure (Fig. 5). Summary of the results are shown in Table 3. As observed form the Table 3, one of the parameters ($\boldsymbol{\delta}$), which depends on stiffness and initial pretension of tethers remains constant for all the postulated failure cases. Other parameter (**q**), which depends on tension variation, differs for various postulated failure. It is also seen from the table that the platform is stable under normal condition (case 1). Even eccentric loads under various postulated failure cases with 5% load amplitude did not result in Mathieu instability. For eccentric loading with 10% load amplitude, cases 2 and 3 show unstable condition, justifying the chaotic nature of tether tension variation. It is interesting to note that under eccentric loads with magnitude of 10% of that of the mass of the platform, when placed on the adjacent buoyant legs (case 4) shows stable condition. This is due to the fact that amplitude of tension variation, which resulted in chaotic nature in the beginning, settles down to lower amplitude. Irrespective of the position of eccentric load considered, platform undergoes Mathieu type instability for eccentric load greater than 10% of total mass of the structure.

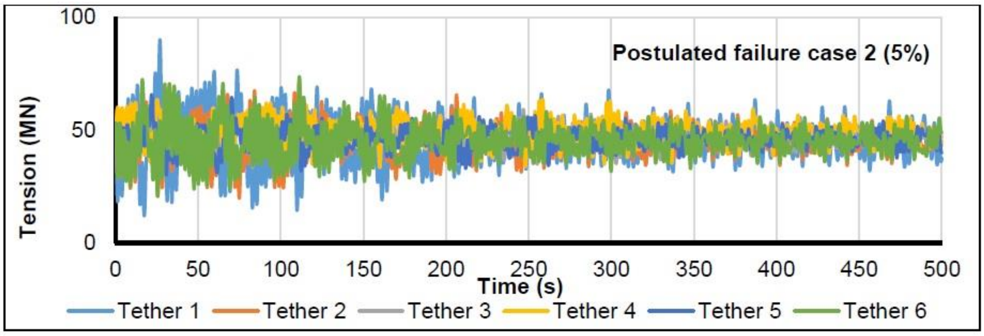

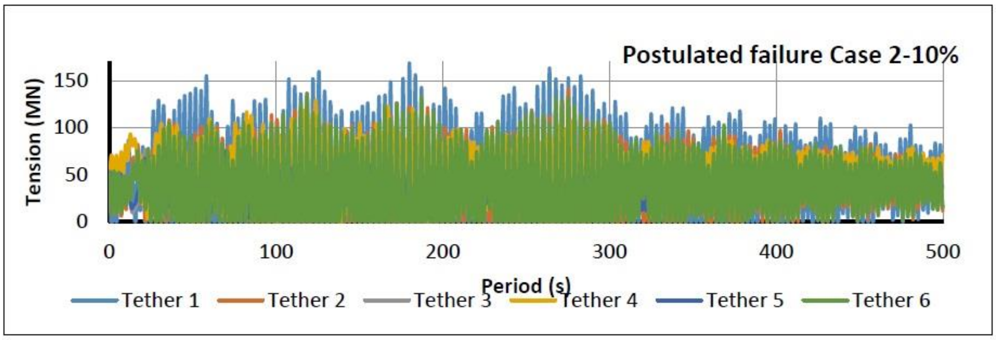

Continued-

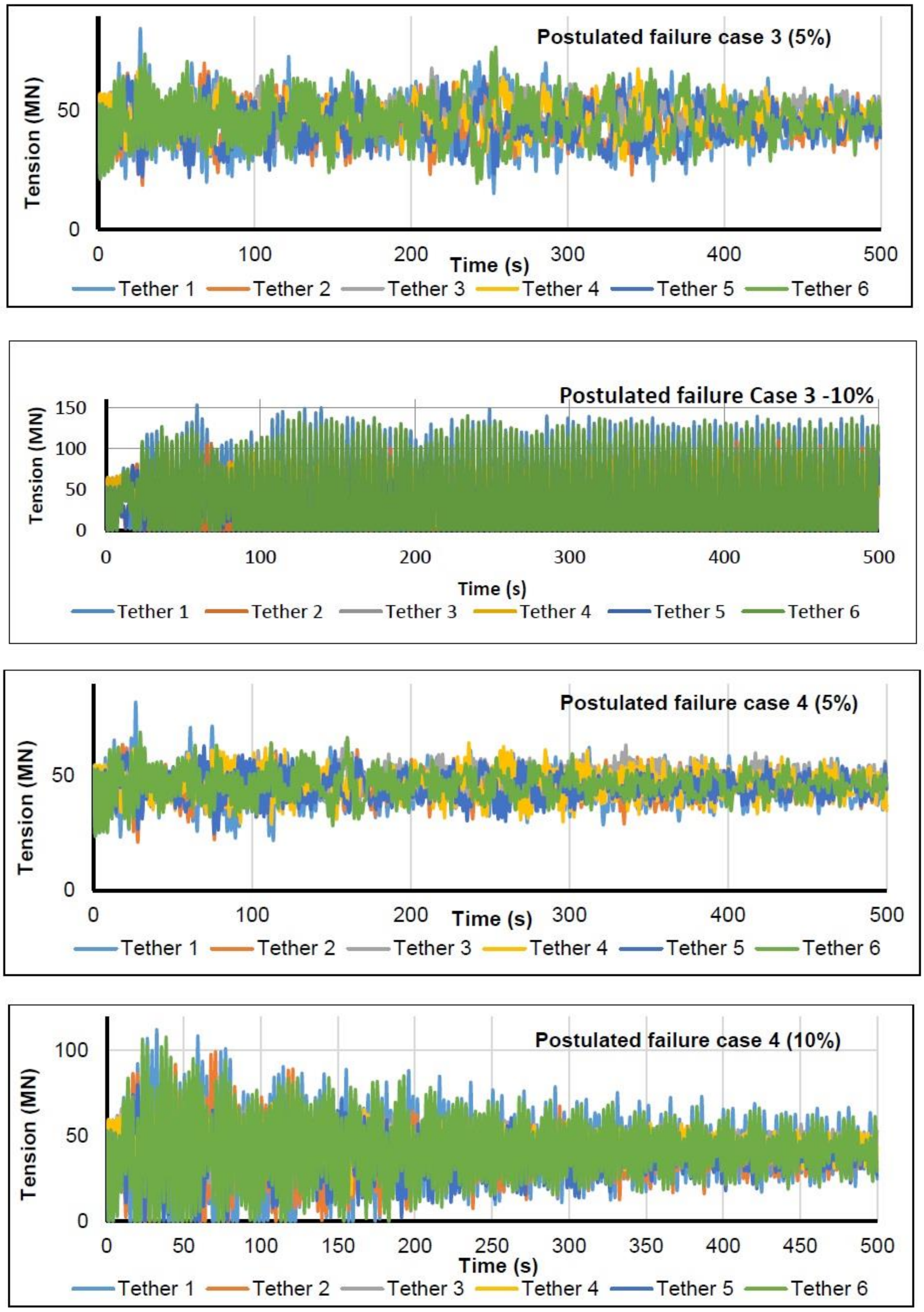

Fig. 4 Dynamic tether tension variation under postulated failure cases

Table 3 Mathieu parameters under postulated failure cases

Description	Load	δ	q	Stability condition
Case 1	-	75.07	5.9	Stable
Case 2	5%	75.07	23.35	Stable
	10%	75.07	73.19	Unstable
Case 3	5%	75.07	20.22	Stable
	10%	75.07	63.6	Unstable
Case 4	5%	75.07	18.49	Stable
	10%	75.07	37.54	Stable (boundary)

5. Fatigue analysis of tethers

Tethers in taut-moored compliant structures are subjected to cyclic loading throughout its life. As seen above, dynamic tether tension variation is significant under the postulated failure cases. Even though the amplitude of tension variation is lesser than that of the tether breaking load, cyclic loading due to environmental loads may lead to fatigue failure (Siddiqui and Suhail 2000, 2001, Hove and Moan 1995). Current study also investigates fatigue life of tethers under axial stress using Miner-Palmgren approach. Fatigue strength is estimated based on the number of cycles (for example, 10^7) for which the maximum stress range that can be applied without causing failure. S-N curve is defined by the following equation

$$A = NS^m \tag{17}$$

where, S is the cyclic stress range, N is the number of cycles to failure, A and m are constants depending on the fatigue class and number of cycles obtained from DNV-RP-C203. While stress range and number of cycles are estimated using Rainflow counting method, Minor's hypothesis is used to obtain the fractional damage caused by different stress range; results are then summed up to obtain overall damage, based on which life of the tether is extrapolated. Damage is given by the following relationship

$$D = \sum_{i=1}^{j} \frac{n_i}{N_i} \tag{18}$$

where, D is total damage, j is number of stress bins, n is number of counts and N is number of stress range. Detailed fatigue analyses are carried out for each tether under the postulated failure cases to obtain service life of tethers. Detailed fatigue analyses are carried out for each tether under the postulated failure cases to obtain overall damage of tethers for 500s, given in Table 4 (tension leg 1 for eccentric loading case3-10%). Summary of results is shown in Table 5. Under normal case a maximum of 34.25 years of life is obtained for tethers were as a minimum of 23.15 years is noted for tethers of wave-entrant buoyant leg. For 5% eccentric loading a maximum reduction of 89.9% in the fatigue life is observed. As seen in cases 2 and 3, for 10% load, fatigue life of tethers is reduced significantly to about 13 days, which is quite alarming. Increase in the magnitude of eccentric loading and position of the load is very important. There is a significant decrease in fatigue life with the increase in the amplitude of tension variation. Very low fatigue life of tethers under Mathieu instability proves the severity of instability. For example, case 4 under 10% loading shows a stable condition but the fatigue life is very low in comparison to other stable condition cases.

Table 4 Damage calculation of tether 1 for case 3-10%eccentric loading for 500s

Stress bin	Counts	Damage
34.76	1	2.70E-08
52.27	1	9.18E-08
69.78	4	8.74E-07
75.62	3	8.34E-07
98.97	1	6.23E-07
110.65	3	2.61E-06
116.49	1	1.02E-06
128.16	1	1.35E-06
134.00	11	1.70E-05
139.84	8	1.41E-05
145.68	11	2.19E-05
151.51	8	1.79E-05
157.35	16	4.01E-05
163.19	20	5.59E-05
169.03	21	6.52E-05
174.86	13	4.47E-05
180.70	15	5.69E-05
186.54	12	5.01E-05
192.38	2	9.15E-06
198.22	2	1.00E-05
204.05	4	2.18E-05
Total damage for 500s		4.32E-04
Life of tethers = 1/ (4.32E-04x7.2x24)[days]		13.4

Table 5 Fatigue life (rounded of) of tethers under eccentric loading

Description	Load	Leg 1	Leg 2	Leg 3	Leg 4	Leg 5	Leg 6	Minimum life
Case 1	-	23 Y	33 Y	33 Y	23 Y	34 Y	34 Y	23 Y
Case 2	5%	2 Y	5 Y	23 Y	13 Y	20 Y	5 Y	2 Y
	10%	14 days	29 days	2 Y	92 days	1 Y	30 days	14 days
Case 3	5%	3 Y	7 Y	15 Y	11 Y	9 Y	4 Y	3 Y
	10%	13 days	45 days	127 days	122 days	51 days	14 days	13 days
Case 4	5%	5 Y	13 Y	14 Y	8 Y	13 Y	9 Y	5 Y
	10%	103 days	286 days	5 Y	4 Y	1 Y	113 days	103 days

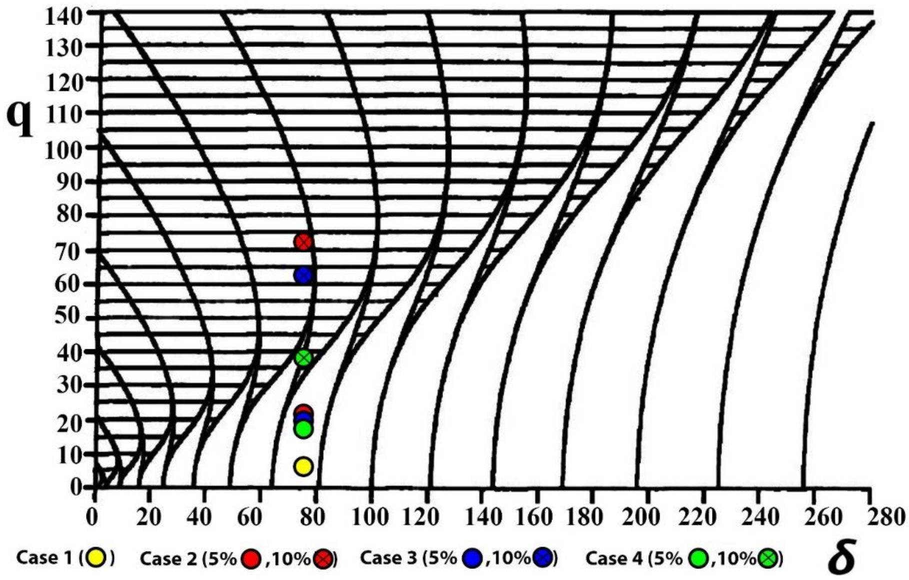

Fig. 5 Mathieu stability for BLSRP under postulated failure cases plotted in extended stability chart given by Patel and Park (1991)

6. Conclusions

Buoyant leg storage and regasification platform is relatively new geometric form of offshore processing platforms. Six buoyant legs, placed symmetrically make the platform insensitive to wave direction and gives better stability. A detailed numerical analysis is carried out for BLSRP using Mathieu equation of stability. Postulated failure cases, created by placing eccentric loads at different locations resulted in dynamic tether tension variation; chaotic nature of tension variation is also observed in few cases. It is observed that the platform is stable under normal conditions. Even eccentric loads under various postulated failure cases with 5% load amplitude did not result in Mathieu instability. For eccentric loading with 10% load amplitude, cases 2 and 3 show unstable condition, justifying the chaotic nature of tether tension variation. Under normal case a maximum of 34.25 years of fatigue life is obtained for tethers where as a minimum of 23.15 years is noted for tethers of wave-entrant buoyant leg. Increase in the magnitude of eccentric load and its position influences fatigue life of tethers significantly. Fatigue life decreases with the increase in the amplitude of tension variation in tethers. Very low fatigue life of tethers under Mathieu instability proves the severity of instability. Mathieu stability analysis of BLSRP under postulated failure has not been attempted before, making the present study innovative.

References

Adrain, B. and Pulido, R.L. (2013), Ship hydrostatics and Stability, Butterworth-Heinemann.
Bowman, F. (1958), Introduction to Bessel functions. Dover, New York.
Chandrasekaran, S. (2015), Advanced Marine structures, CRC Press, Florida, ISBN 9781498739689.

Chandrasekaran, S. (2016a), Offshore structural engineering: Reliability and Risk Assessment. CRC Press, Florida, ISBN:978-14-987-6519-0.

Chandrasekaran, S. (2017), Dynamic analysis and design of ocean structures, Springer, 2nd Ed., Singapore.

Chandrasekaran, S. and Jain, A. (2016), Ocean structures: Construction, Materials and Operations, CRC Press, Florida, ISBN: 978-14-987-9742-9.

Chandrasekaran, S. and Kiran, P.A. (2017), "Mathieu stability of offshore triceratops under postulated failure", *Ship. Offshore Struct.*, **13**(2), 143-148

Chandrasekaran, S. and Lognath, R.S. (2017), "Dynamic analyses of Buoyant leg Storage and Regasification platforms: Numerical studies", *J. Mar. Syst. Ocean Tech.*, **12**(2), 39-48.

Chandrasekaran, S. and Lognath, RS. (2015), "Dynamic analyses of Buoyant Leg Storage Regasification Platform (BLSRP) under regular waves: Experimental investigations", *Ship. Offshore Struct.*, **12**(2), 171-181.

Chandrasekaran, S. and Madhuri, S. (2012a), "Free vibration response of offshore triceratops: Experimental and analytical investigations", *Proceedings of the 3rd Asian Conf. on Mech. of Functional Materials and Struct.*, 8-9 Dec, New Delhi.

Chandrasekaran, S. and Madhuri, S. (2012b), "Stability studies on offshore triceratops", *Proceedings of the Tech Samudhra Int. Conf. on Tech. of Sea*, Indian Maritime University, Vishakapatnam, India, **1**(10), 398-404.

Chandrasekaran, S., Chandak, N.R. and Gupta, A. (2006), "Stability analysis of TLP tethers", *Ocean Eng.*, **33**(3-4), 471-482.

Chandrasekaran, S., Lognath, R.S. and Jain, A. (2015), "Dynamic analysis of buoyant leg storage and regasification platform under regular waves", *Proceedings of the 34th Int. Conf. on Ocean, Offshore and Arctic Engineering*, St. John's, NL, Canada, May 31-June 5.

Chandrasekaran, S., Madhuri, S. and Gaurav, A.K. (2010), "Dynamic response of offshore triceratops under environmental loads", *Proceedings of the Int. Conf. of Marine Tech.*, 11-12, Dec, Dhaka, Bangladesh.

Chandrasekaran, S., Mayank, S. and Jain, A. (2015), "Dynamic response behavior of stiffened triceratops under regular waves: Experimental investigations", *Proceedings of the 34th Int. Conf. on Ocean, Offshore and Arctic Engineering* , St. John's, NL, Canada, May 31-June 5.

Chandrasekaran, S., Sundaravadivelu, R., Pannerselvam, R. and Madhuri, S. (2011), "Experimental investigations of offshore triceratops under regular waves", *Proceedings of the 30th Int. Conf. on Ocean, Offshore and Arctic Engg*, Rotterdam, The Netherlands, 19-24th June.

Chandresekaran, S., Madhuri, S. and Jain, A. (2013), "Aerodynamic response of offshore triceratops", *Ship. Offshore Struct.*, **8**(2), 123-140.

Copple, R.W. and Capanoglu, C.C. (1995), "Buoyant leg structure for development of marginal fields in deep water", *Proceedings of the 5th Int. Offshore and Polar Engineering Conf.*, The Hague, The Netherlands, June 11- 16.

Goldstein, S. (1929), "Mathieu functions", Trans. Cambridge Philosophical Society, **23**, 303-336.

Haslum, H.A. and Faltinsen, O.M. (1999), "Alternative shape of spar platforms for use in hostile areas", *Proceedings of the 31st Offshore Technology Conference*, Houston, (OTC 10953).

Hove, G.O. and Moan, T. (1995), "Fatigue and fracture reliability of TLP tether system before and after failure", *Proceedings of the 7th ICASP, Applications of statics and Probabalilty*, (1). Rotter-dam: Balkema.

Ince, E.L. (1925), "Researches into the characteristic numbers of the Mathieu equation", *Proc. Royal Society of Edinburgh*, **46**, 9-20.

Jefferys, E.R. and Patel, M.H. (1982), "Dynamic analysis models of Tension Leg Platforms", *J. Energ. Resour. Technol.*, **104**, 217- 223.

Koo, B.J., Kim, M.H. and Randall, R.E. (2004), "Mathieu instability of a spar platform with mooring and risers", *Ocean Eng.*, **31**(17-18), 2175-2208.

Mclachlan, N.W. (1947), Theory and application of Mathieu functions, Oxford university press.

Patel, M.H. and Park, H.I. (1991), "Dynamics of tension leg platform tethers at low tension. part I - Mathieu stability at large parameters", *Mar. Struct.*, **4**(3), 257-273.

Perrett, G.R. and Webb, R.M. (1980), "Tethered Buoyant platform production system", *Proceedings of the 12th Annual Offshore Tech. Conf.*, 3881, Houston, Texas, 5-8th May.
Rho, J.B. and Choi, H.S. (2004), "Vertical motion characteristics of truss spars in waves", International Society of Offshore and Polar Engineers, 662-665
Rho, J.B., Choi, H.S., Lee, W.C., Shin, H.S. and Park, I.K. (2002), "Heave and pitch motion of a spar platform with damping plate", *Proceedings of the 12th International Offshore and Polar Engineering Conference*, Kitakyshu.
Rho, J.B., Choi, H.S., Lee, W.C., Shin, H.S. and Park, I.K. (2003), "An experimental study for mooring effects on the stability of spar platform", *Proceedings of the 13th International Offshore and Polar Engineering Conference*, Honolulu, HI.
Rho, J.B., Choi, H.S., Shin, H.S. and Park, I.K. (2005), "A study on Mathieu-type instability of conventional spar platform in regular waves", *Int. Soc. Offshore Polar Engineers*, **15**(2), 104-108
Siddiqui, N.A. and Suhail, A. (2001), "Fatigue and fracture reliability of TLP tethers under random loading", *Mar. Struct.*, **14**(3), 331-352.
Siddiqui. N.A. and Suhail, A. (2000), "Reliability analysis against progressive failure of TLP tethers in extreme tension", *Reliab. Eng. Syst. Safe*., **68**(3), 195-205.
Simos, A.N. and Pesce, C.P. (1997), "Mathieu stability in dynamics of TLP tether considering variable tension along the length", *T. Built Environ.*, **29**, 175-186.
White, C.N., Copple, R.W. and Capangolu, C. (2005), "Triceratops: An effective platform for development of oil and gas fields in deep and ultra-deep water", *Proceedings of the 15th Int. Offshore and Polar Eng. Conf*., Seoul, Korea, June 19-24.

MK

Nomenclature

M	Total mass of tether
$T(x)$	Total tension in tether
$B\mathrm{v}$	Viscous damping coefficient
P	Pretension
μ	Physical mass per unit length
L	Length of tether
a	Tension amplitude
ω	Wave frequency
η, $\boldsymbol{\beta}n$	Variables
J_0, Y_0	Bessel functions
$\boldsymbol{\delta}$, q	Mathieu parameters
ω_n	Modal wave frequency
$\boldsymbol{\tau}$	Dimensionless time variable
$Xn(x)$	modal forms for tether dynamics model
f	lateral displacement of tether
A, m	constants for S-N curve obtained from DNV-RP-C203
N	number of cycles to failure
D	total damage
j	number of stress bins
n	number of counts